Finite-element modeling and analysis of time-dependent thermomechanical distortion of optical sheets in a LCD module

Jae-Won Lee*, Hak-Mo Hwang, and In-Jae Chung
LCD R&D Center, LG.Philips LCD, 533, Hogae-dong, Dongan-gu, Anyang-shi, Gyongki-do, 431-080, South Korea
Phone: 82-31-450-7474, E-mail: jwonlee09@lgphilips-lcd.com

Abstract

Each type of optical sheets in a LCD module experiences a characteristic behavior for thermal loading and unloading. During thermal cycling, a polymeric behavior is reversible and recyclable, depending on a material stiffness critically affected by temperature and time. Some critical issues on temperature- and time-dependent themomechanical deformation of the polymeric sheet are addressed by finite-element thermal results, followed by structural simulation results in this study.

1. Objectives and Background

Various types of optical sheets, i.e., films and plates, are applied in LCD modules for IT (Information Technology) and CE (Consumer Electronics). All of them are thermoplastics reversible/recyclable during thermal cycling; each of the optical sheets has a characteristic morphology, and so its structural behavior critically depends on a specific thermal condition within the LCD module (LCM). For each of LCM components including the optical sheets, the thermal condition subject to LCM driving is defined as a temperature change for a specific duration of time. Temperature changes of the optical sheets, induced by a light source in the direct/side-light-type LCM, causes thermomechanical deformation that ultimately affects display quality of the LCM.

Thermal cycling in LCM driving can be described by a temperature profile with respect to a time. It can be classified into thermal loading and unloading; thermal loading is reclassified into heating and dwelling. Heating is the first temperature range of a temperature profile, in which the LCM is warmed-up by heat emitted from a light source (up to a system-off state). Dwelling is the second temperature range, in which the LCM is thermally saturated by an increased duration of system-on. Just after shutting off the LCM power, an inside temperature of the LCM is gradually decreased by a reaction to the ambient air surrounding the LCM. Cooling by convection is the last temperature range of the temperature profile, in which the LCM (or all the LCM components) is in the thermal-unloading state.

A physical phase of the thermoplastic for thermal loading is generally classified into five states: glassy (or crystalline), leathery, rubbery, rubbery plateau, and finally viscous state, and vice versa for thermal unloading. Approaching the leathery state, the thermoplastic experiences a significant increase in reversible (or elastic) and irreversible (or plastic or residual) strain at temperatures above the glass transition temperature (T_g). As a primary issue of this study, a permanent expansion in dimension, which is caused by irreversible strain, initially appears in the optical sheet in this range.

Identifying and quantifying such a thermally induced micron-scale polymeric behavior is very difficult, using experimental tools and related methods, because a boundary between the physical phases is not clear. Preferably, developing a simulation program for prediction is considerably desirable and effective for ultimate improvement of quality reliability and productivity. This concept uses conventional optical sheets generally used in the LCMs, followed by thermal cycling until the mechanical response of an optical sheet produces a residual deformation at a transitional state between the glassy and the leathery. The simulation program consisting of structural and thermal processes is stable and robust, which is based on the finite-element (FE) method (i.e., ANSYS® as a commercial modeling software). It addresses some critical issues on a characteristic behavior of the optical sheets in the LCM by modeling effects of principal factors: e.g., material property, dimension, shape, initial/boundary/restricted condition, and thermal processing condition, etc.

2. Results

2.1. Overview

To analyze the temperature- and time-dependent thermomechanical deformation of the optical film, two FE models were developed. The first FE thermal model is used to obtain a temperature profile of the diffuser film as a temperature-time relationship in the typical thermal loading and unloading steps. The first step is sheet (a diffuser film) heating by a diffuser plate at a temperature specified by CCFLs (Cold Cathode Fluorescent Lamps) as a light source, the second is sheet dwelling at a constant temperature, and the last is sheet cooling just after putting out the lamps. The second model simulates structural response of the diffuser film based on the thermal results by the first model. Parametric studies include the structural response corresponding to the various simulated temperature profiles during thermal cycling.

2.2. FE Thermal Analysis

Figure 1 shows a 23-inch backlight unit (BLU) that is simplified for computational efficiency: i.e., a diffuser film, a diffuser plate, twelve lamps, electrical parts, and a case for mechanical shielding, respectively.

Fig. 1. Photograph of a 23-inch backlight unit for FE modeling and analysis.

Figure 2 is a schematic of the three-component heat transfer system based on Fig. 1., and dimensions of the corresponding components are included in Table 1.

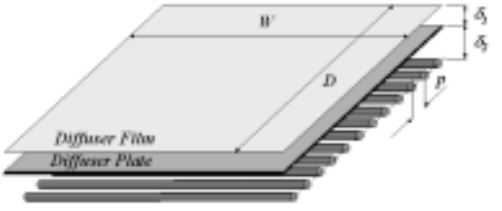

Fig. 2. Model geometry of the three-component heat transfer system: a diffuser film, a diffuser plate, and twelve CCFLs

All the lamps are uniformly arrayed at a pitch of 25.0 mm. The diffuser film is kept at a proximity gap (initially, δ_1 = 100 μm) from the top surface of the diffuser plate at an initial state (time t = 0 sec.) for a reference temperature (T_{Ref}) of 25 °C. An initial gap (δ_2), filled with an ambient air, between the diffuser plate and the lamp is 9.8 mm.

Table 1. Dimensions of the optical sheets (units: m)

	W	*D*	*Thickness*
Diffuser film	0.525	0.325	0.2E-3
Diffuser plate	0.525	0.325	2.0E-3

As shown in Fig. 3, a thermocouple is equipped to measure the top-surface temperature of a lamp at a specific position: the total number of thermocouples is 7 for a unit lamp, and so 84 for the BLU, which is optimized for minimizing a total quantity of thermocouples needed.

Fig. 3. Thermocouples equipped along the top surface of the each lamp: K-type, MV200 for mobile coding.

Figure 4 shows a temperature profile of each of the lamps at the position of y = 17.5, 167.5, and 292.5 mm, respectively, just after 90 minutes for an arbitrary input condition, i.e., 24V and 2.55A, of driving the LCM. The relative increases of the temperature around each end of the lamp are due to effects of electrodes at the corresponding positions.

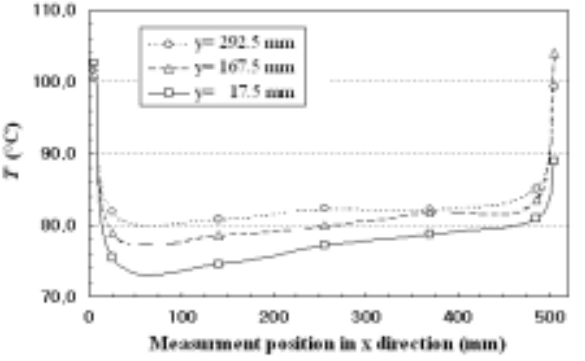

Fig. 4. Plot of temperature variation of the lamp along x-axis at y = 17.5/167.5/292.5 mm just after 90 mins.

Figure 5 is an equivalent temperature profile of the diffuser plate considering a temperature increase of the air surrounding the LCM; all the data are measured at the corresponding positions separated by a gap of δ_2 from each of the lamps just after 90 minutes.

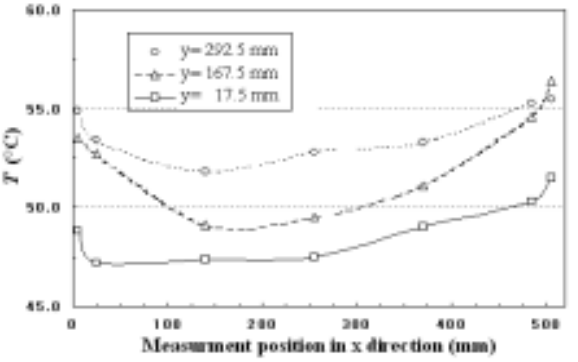

Fig. 5. Plot of a temperature profile of the diffuser plate at the same position corresponding to each of the lamps just after 90 mins.

Figure 6 shows the FE thermal model without any non-flatness at time $t = 0$ for the heat transfer system illustrated in Fig. 2.

Fig. 6. FE thermal model for the two-component heat transfer system.

One of the primary factors inducing nonlinearities of a polymeric behavior is temperature dependence of material properties. Based on the preliminary FE thermal results, the most influential thermal properties are thermal conductivity (k) and specific heat capacity (C_p), but their temperature dependence in this study has no significant effect on the overall temperature profile of the diffuser film, as based on the aspect ratio: thermal properties of the diffuser plate as a heat source has no meaning (Table 2).

Table 2. Fixed thermal modeling parameters

	Units	Diffuser film	Diffuser plate
k	W/m-K	0.33	0.21
C_p	J/kg-K	2,260	1,486

Heat transfer between the two optical sheets is conduction or convection or both, mainly depending on a proximity gap. Convection around the diffuser film is defined as buoyancy-driven free flow: radiation can be neglected, due to a temperature difference (corresponding to the pre-defined gap δ_1).

The variable heat transfer coefficient (h) between the upper surface (or lower surface) of the diffuser film and the extensive surrounding air (or enclosed air in the proximity gap) can be induced from the two dimensionless numbers, the Rayleigh number (Ra) and the Nusselt number (Nu).

$$Ra = \frac{g \cdot CTE \cdot (T_{Film} - T_{Air}) \cdot l^3}{\nu\alpha} \qquad \text{(Eq. 1)}$$

$$Nu = \frac{h \cdot l}{k} \qquad \text{(Eq. 2)}$$

in which g is the gravitational acceleration (≅ 9.8 m/s^2), CTE is the coefficient of thermal expansion, l is a characteristic length of the geometry, ν is the kinematic viscosity, α is the thermal diffusivity, and k is the thermal conductivity. In addition, T_{Film} is a mean temperature of the diffuser film and T_{Air} is a temperature of the surrounding air. As shown in Fig. 7, h becomes a function of temperature by applying Eqs. (1) and (2) to the following correlation:

$$Nu = C \cdot Ra^n$$

in which C and n are empirical engineering constants: e.g., laminar flow ($10^4 \le Ra \le 10^7$) for a temperature range of 25~100 °C, and then $C = 0.54$, $n = 0.25$ at the top surface [1], [2].

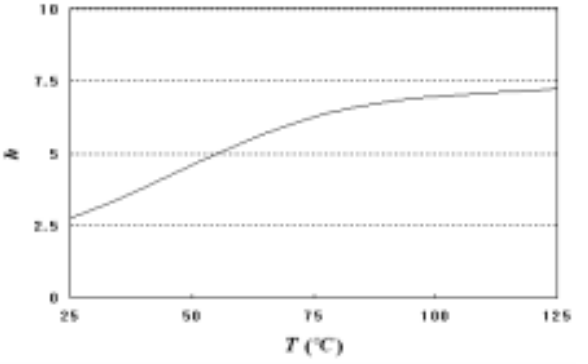

Fig. 7. Temperature-dependent heat transfer coefficient at the top surface of the diffuser film.

Including the thermal conductivity shown in Fig. 8, each of the heat transfer coefficients at the top and the bottom of the diffuser film are applied to the FE simulation program as a function of temperature after curve fitting [3], [4], [5].

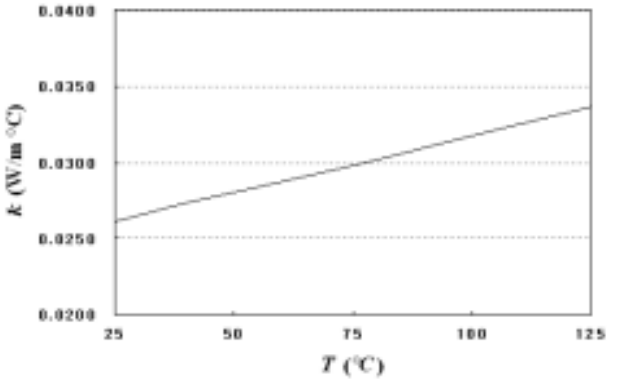

Fig. 8. Plot of the variable thermal conductivity of the air.

In order to validate the thermal simulation program, one-dimensional heat flow is arbitrarily defined: i.e., the diffuser plate at a uniform temperature of 100 °C during 180 seconds using all the specifics mentioned above. Especially, some specifics of the diffuser film are arbitrarily defined for more effective visualization of the corresponding temperature profile.

Shown in Fig. 9 is the temperature profile of the diffuser film, in which the numerical result has a maximum error of 0.67% at 46.6 seconds as compared with the theoretical [6], [7].

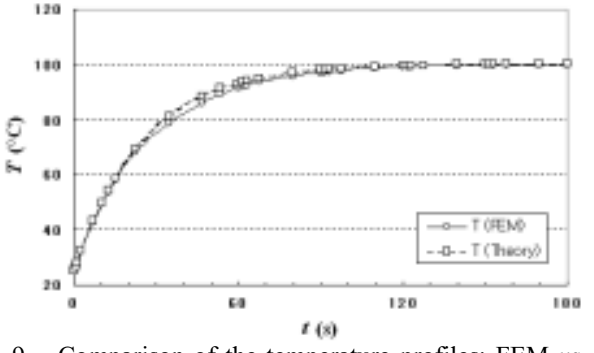

Fig. 9. Comparison of the temperature profiles: FEM *vs.* Theory.

Figure 10 shows variation of the final temperature corresponding to a change of the proximity gap spacing between the diffuser film and the diffuser plate for the same condition defined in Fig. 9.

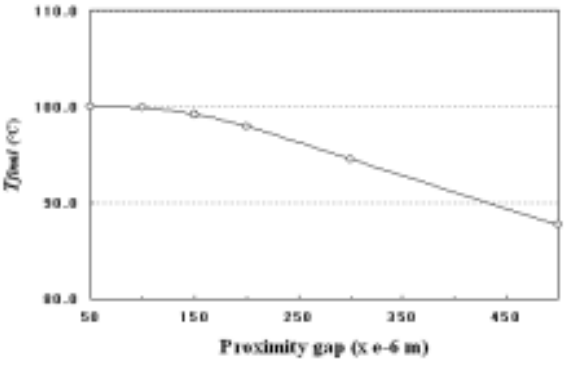

Fig. 10. Plot of variation of the final temperature of the diffuser film corresponding to a change of the proximity gap.

For the specifics initially defined above, Fig. 11 shows a temperature contour over the diffuser film at the time of 90 seconds, in which a maximum temperature difference based on the reference temperature of 25 °C is 9.7 °C. This kind of a temperature difference basically causes nonuniformity in luminance over the BLU surface, and then critically affects a display quality of the LCM.

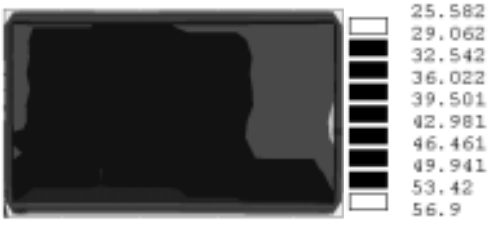

Fig. 11. Temperature contour of the diffuser film at 90 sec.

2.3. FE Structural Analysis

As mentioned earlier in 2.1, FE structural modeling simulates polymeric response of the diffuser film based on the FE thermal result in Fig. 11. The diffuser film in the BLU initially is in the glassy state (solid phase) on its (relaxation or viscoelastic) modulus-temperature curve at the reference temperature. Accordingly, FE structural simulation includes two different behavioral regimes that induce a significant deformation of the diffuser film: i.e., elastoplastic (or fully-developed plastic) around T_g and viscoelastic above T_g. Figure 12 illustrates the basic structure of the simulation program that is applicable to the both behavioral regimes for thermal loading and unloading. In general, however, all kinds

of the optical sheets applied in the LCM have basic characteristics that resist being deformed.

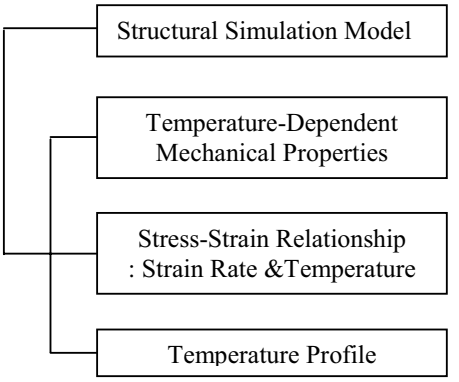

Fig. 12. Physical modeling parameters on structural behavior.

As described in Fig. 12, all the parameters are correlated. The principal temperature-dependent mechanical properties affecting thermomechanical deformation of the diffuser film are the modulus, the static yield stress, the coefficient of thermal expansion, and the surface tension. In addition, the stress-strain-temperature relationship induces combined nonlinearities (material, geometry, boundary, and all combined) of the optical film during thermal cycling. The strain rate parameters affecting the stress-strain relation significantly dominate a time-dependent structural behavior after the glassy state.

Figure 13 shows an equivalent strain over the diffuser film at time t = 90 seconds, which is based on the temperature profile as a thermal FE result shown in Fig. 11. Only for thermal loading, the structural FE modeling includes an effect of the gravity.

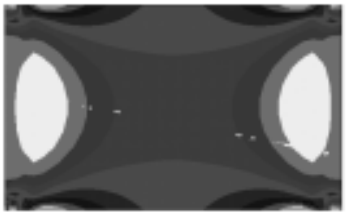

Fig. 13. Plot of an equivalent strain over the diffuser film at t = 90 sec.

Both the modulus and the yield stress, as functions of temperature and time, are the most influential material properties driving relaxation during thermal loading. They vary with temperature up to the flow temperature. In addition, the surface tension, which is defined as the reversible work for creation of a unit surface area at constant temperature, pressure, and chemical composition, linearly varies with temperature. The effects of the coefficient of thermal expansion are decreased around T_g.

2.4. Summary and Conclusions

As based on the thermal simulation results, the temperature profile is primarily affected by the two temperature-dependent material properties such as the thermal conductivity and the specific heat capacity: in addition, the proximity gap spacing between the components is the most influential factor determining the slope of the temperature profile at the transition state. Thermomechanical behavior corresponding to the temperature profile completely depends on the characteristic glass transition temperature of the polymeric sheet. It is also subject to the temperature-dependent mechanical properties: i.e., a modulus, a yield stress, a coefficient of thermal expansion, and a surface tension. Individual and/or combined effects of all the factors on the both thermal and structural FE results will be additionally investigated. Thus, both programming issues on modeling efficiency and accuracy are inclusively improved by enhancing the current program through continuous comparison of theoretical and experimental results.

3. Impact

As briefly mentioned earlier, the thermal simulation result is compared with the theoretical result only for the one-dimensional heat flow. The simulation program with theoretical validity can be extended to two-and three-dimensional behaviors to realize the actual behavior of the optical sheet. It can be effectively utilized to investigate optimized material properties for development of the optical sheets for LCMs with more increased quality and reliability.

4. References

[1] R. J. Goldstein, E. M. Sparrow, and D. C. Jones, “Natural Convection Mass Transfer Adjacent to

Horizontal Plates," Int. J. Heat Mass Transfer, 16, 1025, 1973.

[2] J. R. Lloyd and W. R. Moran, "Natural Convection Adjacent to Horizontal Surfaces of various Planforms," ASME Paper 74-WA/HT-66, 1974.

[3] American Society of Heating, Refrigerating, and Air Conditioning, "ASHRAE Hanbook of Fundamentals," ASHRAE, New York, NY, 1981.

[4] J. Brandup et al., editors, "Polymer Handbook," 4th ed., Vol. 1, Wiley, New York, NY, 1999.

[5] N. B. Vargaftik, "Tables of Thermophysical Properties of Liquids and Gases," 2nd ed., Hemisphere Publishing, New York, NY, 1975.

[6] W. H. McAdams, "Heat Transmission," 3rd ed., McGraw-Hill, New York, NY, 1954.

[7] N. Ramanan, F. F. Liang, and J. B. Sims, "Conjugate Heat-Transfer Analysis of 300-mm Bake Station," Proceedings of SPIE, Vol. 3678, pp. 1296-1306, 1999.